



SAKARYA ÜNİVERSİTESİ

FEN BİLİMLERİ ENSTİTÜSÜ DERGİSİ

Sakarya University Journal of Science
SAUJS

ISSN 1301-4048 | e-ISSN 2147-835X | Period Bimonthly | Founded: 1997 | Publisher Sakarya University |
<http://www.saujs.sakarya.edu.tr/>

Title: Production Methods Effect on Nanosilica Properties

Authors: Aysu AYDINOĞLU, Büşra ÖZTÜRK, Afife Binnaz HAZAR YORUÇ

Received: 21.12.2022

Accepted: 17.09.2023

Article Type: Research Article

Volume: 27

Issue: 6

Month: December

Year: 2023

Pages: 1286-1299

How to cite

Aysu AYDINOĞLU, Büşra ÖZTÜRK, Afife Binnaz HAZAR YORUÇ; (2023), Production Methods Effect on Nanosilica Properties. Sakarya University Journal of Science, 27(6), 1286-1299, DOI: 10.16984/saufenbilder.1220994

Access link

<https://dergipark.org.tr/en/pub/saufenbilder/issue/80994/1220994>

New submission to SAUJS

<http://dergipark.gov.tr/journal/1115/submission/start>

Production Methods Effect on Nanosilica Properties

Aysu AYDINOĞLU¹ , Büşra ÖZTÜRK*¹ , Afife Binnaz HAZAR YORUÇ¹ 

Abstract

This study explored nanosilica synthesis using colloidal silica, silica sand, and TEOS, utilizing rotary evaporator drying, sol-gel, and titration methods. It examined the influence of these techniques on silica's functionalization and mechanical properties. Methacryloxypropyl trimethoxysilane was employed for silanation, with silica characterized using various analytical methods. Particle sizes from SEM images were 19 nm and 14 nm for rotary and sol-gel samples, respectively, while titration samples showed an irregular structure. Zetasizer analysis revealed larger particle sizes. The purity of silica powders ranged from 90% to 99%, and titration samples demonstrated the highest silanability. When used in dental composites, rotary-evaporated silica displayed promising suitability based on its mechanical and physical properties.

Keywords: Silica nanoparticles, silanization, sol-gel, titration, rotary evaporator drying

1. INTRODUCTION

Dental resin composites primarily comprise a silane-modified inorganic filler and an organic matrix [1]. The polymerization process occurs within the dental cavity in the presence of oxygen and water. However, these composites can have cytotoxic effects due to the release of free monomers during monomer-polymer conversion. Therefore, reducing the resin ratio by increasing the amount of inorganic fillers is considered an effective approach to minimize the toxicity of oral cells in contact with restorations [2].

Moreover, incorporating a high level of inorganic particulate reinforcing fillers is essential to enhance the mechanical properties of dental fillers, particularly for

posterior restorations. Pretreatment, such as silanization of the inorganic matrix, is necessary to ensure proper dispersion and high filler content.

Notably, the development of technology has introduced significant materials, including nano-silica, nano-hydroxyapatite (n-HAP), and carbon nanotubes (CNT). Silicon (Si) is the second most abundant element in the Earth's crust, primarily found in the form of silica in rocks. Silica is frequently used as an additive material in numerous studies due to its large surface area, stable composition, chemical inertness, non-toxicity, modifiable structure, resistance to organic solvents, thermal stability, easy availability, and low cost [3].

* Corresponding author: busraoztrk@gmail.com (B. ÖZTÜRK)

¹ Yıldız Technical University, Türkiye

E-mail: aysuaydn@yildiz.edu.tr, yoruc@yildiz.edu.tr

ORCID: <https://orcid.org/0000-0002-1875-2249>, <https://orcid.org/0000-0002-2250-8134>, <https://orcid.org/0000-0001-7281-2305>



Silica particles are often modified with suitable functional groups to enhance the mechanical properties of dental composite fillings [4]. This modification involves covalent bonding or interactions, such as hydrogen bonding and Van der Waals forces, between various functional groups and the silanol groups present on silica particles' surfaces [5]. Nano-silica and silanized nano-silica have found extensive use in aesthetic restorative treatments in recent years.

Dental restorations are multi-phase materials with a complex microstructure, comprising one or more interfaces. The characteristic feature of sharp interfaces is observed in amalgam, resin-based, macro-sized glass, or ceramic-filled composites. Silane coupling agents, frequently employed in dental restorations, enhance the interfacial connection between the organic and inorganic matrices in composites. They also reduce viscosity during the process, alter surface catalytic effects, and improve the dispersion of particulate fillers. Silanization is a traditional approach used to enhance the surface properties of silica particles. It involves chemically connecting the silanol groups on the silica surface to silane molecules through chemical reactions.

Various factors, such as pH, concentration, organofunctional groups, solvent, application method, and temperature of the silane solution, influence the interfacial structures of the silane coupling agent. In a given resin/filler system, the physicochemical nature of the silane coupling agents (chemical structure, molecular size, hydrophobicity, reactivity, functionality), the silanization procedure employed, and the resulting silane layer orientation and degree significantly impact the physicochemical and mechanical properties of the interphase and, consequently, the composite [6]. The durability of the interface in the oral environment and its ability to transfer stresses during chewing are vital characteristics of dental composites. Silanized silica using Methacryloxypropyl trimethoxysilane (A-

174) silane aims to improve the quality and durability of the filler/matrix interface [7].

Within the scope of this study, nano-silica will be synthesized and utilized as a supporting phase in dental composite fillings. The intermediate phase, derived from an organosilane called silane coupling agents, is designed to chemically bond with the matrix and filler phases. Compared to conventional composites with micro-sized fillers, the interphase's impact on the physico-mechanical properties is more pronounced in nanocomposites. These fillers possess an extremely high surface-to-volume ratio, necessitating higher levels of silanization. A-174 will be used as the silane coupling agent in this study [8-9].

In recent years, various production methods have been developed for nanoparticle synthesis. However, two methods have been used consistently from the past to the present. One of these methods is the Stöber method, which involves a sol-gel process consisting of hydrolysis and condensation reactions of tetraethyl orthosilicate (TEOS) in alcohol, water, and ammonia mixtures.

The other method is the microemulsion method, which utilizes a single-phase system comprising three main components [10-11]. In this study, nano-sized silica will be synthesized using a titration process with natural silica sand and the drying of commercial Ludox Colloidal silica, in addition to the sol-gel process [12].

1.1. Experimental

1.1.1. Synthesis of silica

Drying of Ludox Colloidal Silica by Rotary Evaporator

A precise amount of 75 mL of colloidal silica (Ludox AS-40, Sigma) is measured using a precision scale. The measured sample is transferred to a 250 mL glass flask and placed inside the R device. The sample is dried for a duration of 3 hours at a temperature of 60 °C

and a rotation speed of 120 rpm in the R device. It is worth noting that in previous studies described in the literature, the dried powders were subjected to grinding using a ball mill. However, for this particular study, the ground samples will not be utilized. Non-milled silica samples exhibit superior properties and smaller particle sizes compared to the milled samples. Therefore, the decision was made to exclude the milled samples from this study [13].

Nanosilica Synthesis by Sol-Gel Method

To obtain silica nanoparticles, the following procedure was followed:

1. Prepare a mixture by adding 21 mL of ethanol (99.9%, Isolab) to 23 mL of pure water (Millipore Simplicity, type 3). Mix the solution using a magnetic stirrer at 60 °C for 10 minutes.
2. Add 0.9 ml of tetraethyl orthosilicate (98% TEOS, Sigma Aldrich) to the solution. Continue stirring the mixture at 60 °C for 20 minutes using a magnetic stirrer.
2. Next, add 50 mL of ammonia (25% NH₃, Isolab) to the solution. Allow the solution to stir in a magnetic stirrer for 1 hour at 60 °C.
4. After 1 hour, remove the solution from the magnetic stirrer and transfer it to a rotary evaporator. Set the R to operate at 105 rpm and 70 °C.
5. Allow the solution to dry in the R under these conditions.
6. Following this procedure, silica nanoparticles can be obtained.

Nanosilica Synthesis by Titration Method

The method used for the preparation of silica nanoparticles from silica sand involves several steps. Here is the procedure:

1. Obtain silica sand (S1-50-300D, Mersin Sand) from Şişecam.
2. Perform calcination on the silica sand to remove the chemical water present in the sand.
3. Wash the calcined sand with pure water. Centrifuge the sand in pure water to allow it to settle at the bottom. Separate the sand from the liquid phase and subject it to calcination again.
4. Wash the calcined and cleaned sand with a 5 M solution of sulfuric acid (95-97% H₂SO₄, Isolab) for 24 hours at 90 °C. Use deionized water for the washing and drying processes.
5. After washing the silica sand with acid, react it in a 30% sodium hydroxide (98% NaOH Pellet, Merck) solution for 30 hours.
6. Filter the mixture to obtain a clarified liquid sodium silicate solution with a pH of 13.7.
7. Conduct titration of the sodium silicate solution at 65 °C using a 15% hydrochloric acid solution. Perform the titration in seven slow steps, each step reducing the pH to about 7 to obtain the silicic acid solution. Between each seven titration steps, carry out six continuous mixing steps, stirring at 300 rpm at 65 °C. Each continuous mixing step should decrease the pH of the sodium silicate solution by 1.
8. Conduct continuous mixing steps for 30 minutes during each mixing step.
9. After completing the titration, continue stirring the silicic acid solution at 300 rpm for 4 hours at 65 °C.
10. Wash the silicic acid solution using deionized water, then dry and mill it.
11. Calcine the silica in an oven at 950 °C to obtain silica nanoparticles.

Following these steps, silica nanoparticles can be obtained from silica sand.

2.1.1. Silanization of silica powder

The modification of inorganic supporting phase systems with organic molecules like silane serves to decrease the hydroxyl groups on the surface of the inorganic phase, resulting in a shift from hydrophilic to hydrophobic properties. Among the silaning agents used in dental composites, 3-methacryloxypropyltrimethoxy silane (MPTMS/A174) is the most preferred. This molecule contains both methoxysilane groups that react with the inorganic supporting phase and methacrylate groups that react with the organic matrix. The following method was carried out under room conditions with a nitrogen atmosphere:

1. Add an appropriate amount of A174 to a sealed glass bottle containing 380 mL of ethanol:water (1:3) solution. Adjust the pH of the solution to 3.5 using an acetic acid solution and mix for 30 minutes.
2. Introduce the supporting phase system to be modified into the solution under vigorous stirring. Mix for 30 minutes on a heated magnetic stirrer, followed by an additional 10 minutes in an ultrasonic water bath.
3. After mixing, reflux the mixture at 80°C for 6 hours.
4. Filter the mixture through filter paper using vacuum filtration. Wash the resulting precipitates with an ethanol/water (1:3) solution to remove any unreacted silane agent.
5. Dry the precipitates in a vacuum oven at 60°C for 24 hours.

The ratio between the amount of silane (X; Eq.1) used as the binding agent and the amount of supporting phase to be treated can

be determined using the equation suggested by Arkles:

$$X = A \times f/\omega \quad (1)$$

Where:

X: Amount of binding agent (g)

f: Amount of supporting phase (g)

A: Surface area of supporting phase (m²/g)

ω: Wetting surface of silane (314 m²/g)

2.1.2. Production of dental composite filling materials

The following steps were undertaken in the process:

1. BisGMA (bisphenol A-glycidyl methacrylate) and UDMA (Urethane dimethacrylate) were heated in an ultrasonic bath at 40°C.
2. BisGMA, UDMA, TEGDMA (triethyleneglycol-dimethacrylate), and HEMA (2-hydroxyethyl methacrylate) were accurately weighed using a precision balance and added to the sample vessel.
3. The prepared organic matrix mixture was supplemented with 60%, 70%, and 75% of the supporting phase, according to the specified ratios.
4. Camphorquinone (0.2%) and 4-EDMAB (0.8%) were added to the mixture. The resulting mixture was then processed in a SpeedMixer device at 2000 rpm for 6 minutes.
5. The composite fillings were allowed to reach room temperature and were then placed in Teflon molds using a spatula.
6. Both sides of the Teflon molds were positioned on a glass plate and secured with clamps.

7. The samples were cured by exposing them to a Blue-LED light device for 20 seconds, resulting in the formation of composite fillings.

Table 1 provides information on the supporting phases utilized in the dental composites, along with their corresponding ratios and code numbers.

Table 1 Supporting phases, ratios and code numbers used in dental composites.

Supportive Phase Type	Supportive Phase Ratio		
	65	70	75
R	C1	C2	C3
R/SA	C4	C5	C6
R/SN	C7	C8	C9
T	C10	C11	C12
T/SA	C13	C14	C15
T/SN	C16	C17	C18
S	C19	C20	C21

2.1.3. Characterization

In the study conducted by Yıldız Technical University, the particle size measurement of nano silica samples was performed using the Zeta-Sizer device (Nano ZS, Malvern). The powders to be measured were mixed with deionized water using an ultrasonic homogenizer for 4 minutes, and a 0.001% (w/v) colloidal solution was prepared. The Zeta-Sizer device was used to measure the particle size in the prepared colloidal solution.

The surface area measurements of the filler phase systems were carried out using the BET (Autosorb-6b, Quantochrome) device. The non-silaned powders underwent a degassing process at 300 °C for 3 hours before the surface area measurements were taken. The surface morphology properties of the silica powders were examined using a Field Emission Scanning Electron Microscope (FE-SEM, Zeiss Sigma 300). The samples were coated with a 20-30 nm thick layer of gold for FE-SEM analysis and analyzed using an energy of 10 kV.

In this study, the wettability degree of silica nanoparticles in the presence of silane (A174) was measured using the capillary rise method. This method involved measuring the increase in liquids with different polarities (water and hexane) over time by monitoring the mass gain. A schematic presentation of the system used for the capillary rise method is shown in Figure 1 of the study. The samples were manually placed in a glass column with a diameter of 4 mm and a height of 10 cm. The column was sealed with a non-woven fabric to support the particle bed. The mass decrease of the container, including the polar (water) or nonpolar (hexane) liquid, was recorded every 5 seconds using an electronic balance. The time $t=0$ corresponds to the moment when the column is submerged in the wetting liquid. It is important to note that the packing of particles and the procedure of the experiment play a significant role in obtaining reliable results. The packing of particles was conducted under the same tapping time and number to ensure consistency.

In the study, after recording the values of mass gain as a function of time, the modified Washburn's equation was used, which incorporates the dependence of mass gain and time [14-15]. The relationship between liquid mass and height in a column is described by Equation 2:

$$m^2 = \frac{C\rho^2\gamma\cos\theta}{\eta} \quad (2)$$

In this equation, "m" represents the mass of the liquid, C is the effective pore diameter, ρ is the density, γ is the surface tension, and η is the viscosity of the liquid.

The 2θ region of the silica supporting phase systems was scanned at 0.02° intervals and 0.5 s/min. X-rays used for scanning were obtained from the Rigaku MiniFlex 600, operating at 40 kV and 15 mA, using a parabolic filter and Cu-K α radiation. The mean crystal size of the supporting phase structures was determined using the Scherrer equation (Equation 3):

$$D = k\lambda/\beta\cos\theta \quad (3)$$

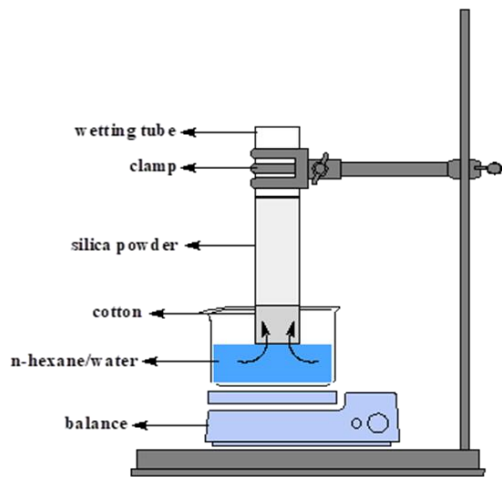


Figure 1 Laboratory set-up used for contact angle measurements by capillary rise method

In this equation, D represents the crystal size in angstroms (\AA) calculated using the (0 0 2) reflection, k is the shape factor (usually taken as 0.9), λ is the wavelength of X-rays (1.54059 \AA for Cu- $K\alpha$ radiation), θ is the angle of reflection for the (0 0 2) plane, and β is half the width of the diffraction peak in radians.

3. CONCLUSIONS AND DISCUSSION

3.1. XRD and ICP Analysis Results of Silica Powders

When examining the XRD spectra of the silica samples in Figure 2, it is observed that the R sample exhibits an amorphous crystal structure, while the T sample exhibits a low cristobalite structure. In Figure 3, the XRD pattern of standard low cristobalite SiO_2 is provided, and the ICSD reference number 01-076-0941 is used. The R sample does not display a regular crystal structure. The T sample, on the other hand, has approximately 99% SiO_2 content. Its crystal phase and cubic lattice parameters are approximately 4.99 \AA on the a-axis, 4.99 \AA on the b-axis, and 7.02 \AA on the c-axis [16]. An additional weak peak is observed at 27.5° , along with a strong

cristobalite peak at 21.8° . These weak peaks seen in Figure 3 have been identified as tridymites (ICDD PDF No. 39-1425).

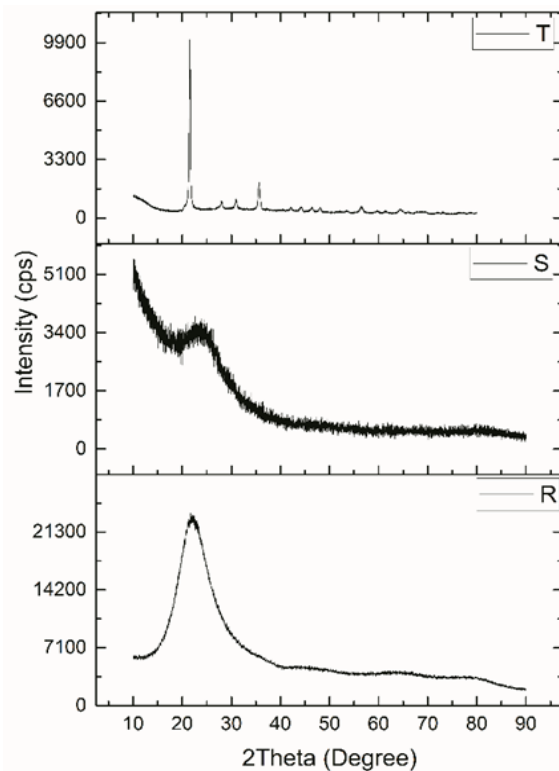


Figure 2 XRD scans of T, S and R Silica structures

According to the Debye-Scherrer equation (Equation 3) and the calculations performed in Figure 4, the crystal size of SiO_2 in the T sample was determined to be 29.928 nm . The β value used in Equation 3 represents the maximum half-full width (FWHM) of the dense peak, and based on this value, the crystal size was calculated to be 29.928 nm .

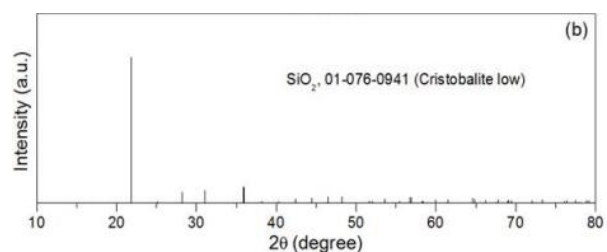


Figure 3 XRD pattern of standard low cristobalite SiO_2 [17]

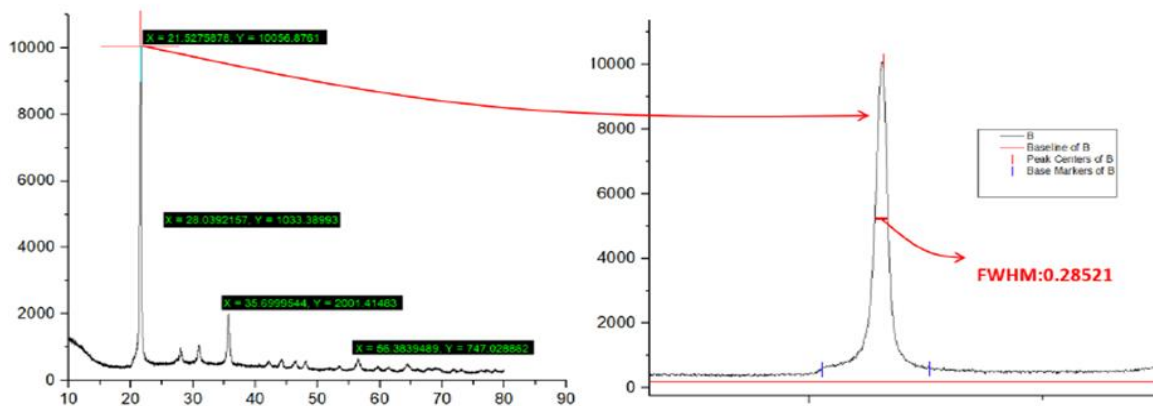


Figure 4 Scherrer plot of T sample

Silica is a mineral component that can contain smaller amounts of other elements such as magnesium, calcium, iron, and aluminum [18]. The average purity values of silica samples obtained through different methods range from 99.25% to 99.48% by weight. Table 2 provides information about the impurities present in silica and their respective ratios.

Table 2 Parameters used in crystal size calculation

Crystal Size Parameters			
k*	λ (Å)	θ	β (FWHM)
0.94	1.54178	21.52	0.28521

*: The K value must be between 0.68 and 2.08. It is usually taken as 0.94.

The developed titration method for silica production is considered environmentally friendly compared to the traditional colloidal silica drying method, and it offers the advantage of lower production costs. The drying process with colloidal silica results in the production of silica with higher purity (Table 3). However, it should be noted that the difference in purity levels is not significant.

3.2. FE-SEM, BET and Zetasizer Analysis Results of Silica Powders

In Figure 5a, FE-SEM images of dried silica samples in the rotary evaporator (R) device are shown. These images reveal that the particle size distribution of the R-coded

sample ranges from 19 to 21 nm. The rotary evaporator device consists of a heating bath, a cooling condenser, a cooling circulator, a vacuum pump, a glass flask for drying the product, and a collection flask. The vacuum pump is a crucial component of the R device as it directly affects the process performance by providing controlled vacuum at appropriate temperature values. Controlled vacuum reduces the vapor pressure of the evaporator system, allowing the solution to evaporate at lower temperatures without disrupting the structure of solvents. Additionally, the vacuum pump lowers the boiling point of the main material, enabling it to separate from the environment without production techniques are provided in Table 4.

Table 3 Impurities and proportions in silica powders

Conc. (ppm)	Rotary Evaporator	Titration	Sol-Gel
Mg	576.1	56.1	195
Al	809.1	1750.1	236
Ca	362.2	19.84	226.3
Fe	142.7	196.9	117
Si	362691.7	270613.0	1521
Total	364581.8	272635.9	2295.3
Si %	99.48	99.25	66.2

It was observed that the surface areas of silica nanoparticles synthesized by the sol-gel method were higher compared to the surface areas of silica nanoparticles dried in the R. During zeta measurements, the particle size of the silica powders was found to be larger than

the particle size obtained from the BET and SEM results. This difference in particle sizes can be attributed to the particles not being stably suspended in the solution. Over time, agglomeration occurs, leading to an increase in particle size. Analyzing the particle distributions based on density (as depicted in Figure 6), it can be observed that all samples

initially have a smaller particle size distribution, but as the particles agglomerate, both the particle size and distribution increase. It is known that the closer the polydispersity (Pdl) value is to zero, the more homogeneous and narrower the particle size distribution is.

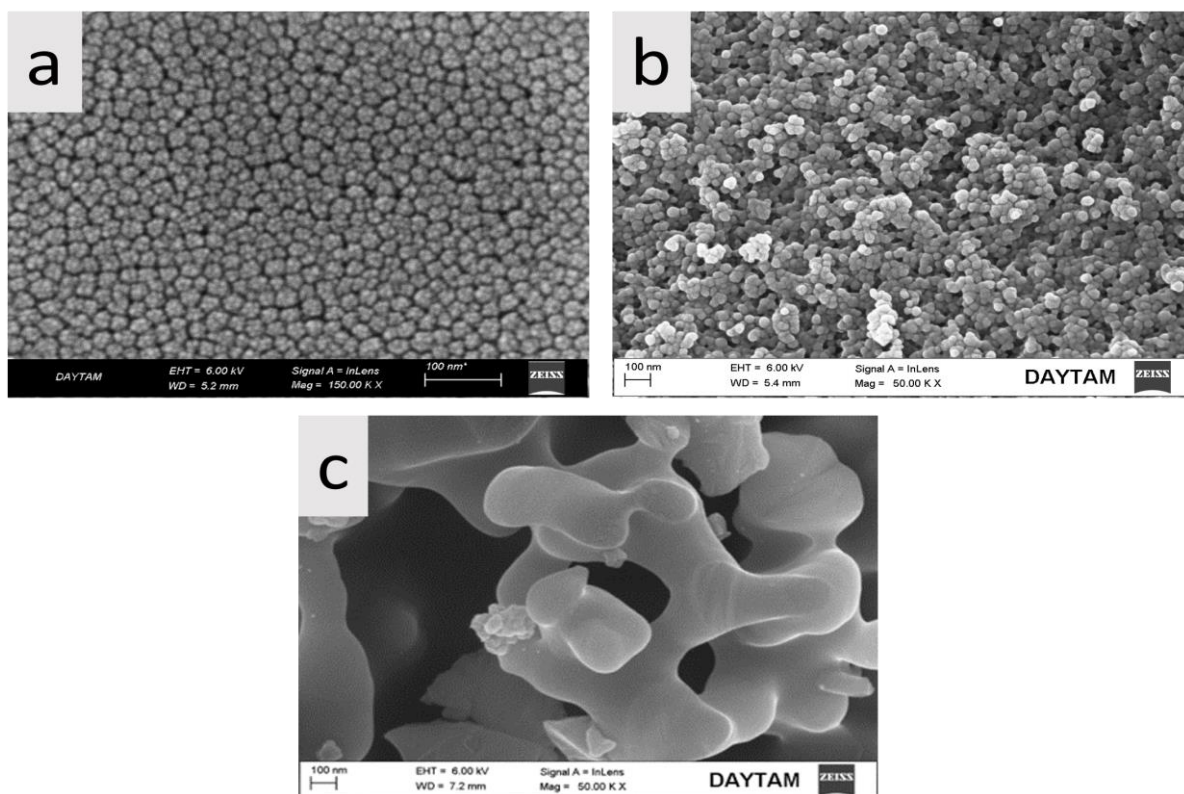


Figure 5 FE-SEM images of silica powders produced by different silica synthesis methods; (a) Rotary Evaporation, (b) Sol-Gel, (c) Titration

Under controlled vacuum, the solvent evaporated by the rotary evaporator passes through the condenser, thanks to the cold environment provided by the cooling circulator's pure water, and condenses in the collection flask. In the R drying process, the centrifugal force and friction between the rotating glass evaporating flask and the liquid sample are utilized. There is no existing literature on silica drying using the R method. It is expected that the rotary evaporator device will minimize agglomeration in nano-silica production. Therefore, it was selected as one of the silica synthesis methods for experimental studies. Silica powder dried with R exhibits a more uniform particle size distribution, indicating that water molecules

are effectively removed from the environment through the R route and result in uniform drying in all directions. Considering the Pdl value of silica powders, sol-gel and titration methods have lower Pdl indices compared to the rotary method. This indicates that silica powders produced with a rotary evaporator have a more homogeneous particle size.

In Figure 5b, FE-SEM images display the S-coded SiO₂ powders produced using the Sol-Gel method. These powders exhibit a grain size ranging from 14 to 30 nm and possess a spherical structure. The S test parameters involved a process temperature of 60 °C. Conducting the process at an elevated temperature increased the surface area and led

to a decrease in particle size. Figure 5c illustrates the FE-SEM images of T-coded silica powders. The ignition temperature of silica powders is 450 °C. Calcination processes conducted above this temperature affected the morphology of the silica particles, resulting in an irregular structure resembling a sea sponge. The porous structure is believed to enhance mechanical adhesion by allowing the organic matrix to settle within the pores. Calcination increased the size of SiO₂ particles, and the particle size was confirmed through Zeta and theoretical particle size analysis. The surface area and grain size properties of the silica supporting phase systems were evaluated. Surface area and particle size measurements of silica powders obtained through different

Table 4 Structural and physical properties of colloidal silica prepared using different synthesis techniques

Structural properties of the primary silica	Structural properties of the primary silica		
	Rotary Evaporation (R)	Sol-Gel (S)	Titration Method (T)
Theoretical particle size (nm)	17	14	-
Zetasizer particle size (nm)	107	181	184
BET surface area, S _{BET} (m ² g ⁻¹)	131	158	0.012
Polydispersity (Pdl)	0.835	0.586	0.575

When examining the Pdl values obtained from the zeta analysis, Figure 6 confirms that silica powders produced via the sol-gel and titration methods have a more homogeneous size distribution compared to the R method. In the case of the R sample, the zeta analysis revealed the lowest particle size. This indicates that the silica powders dried using the rotary evaporator exhibit a lower tendency for agglomeration compared to other silica powders. The rotational movement of the powders during drying in accordance with the

principles of the rotary evaporator contributes to this reduced agglomeration tendency. The rotational movement ensures homogeneous drying and minimizes the particle size distribution.

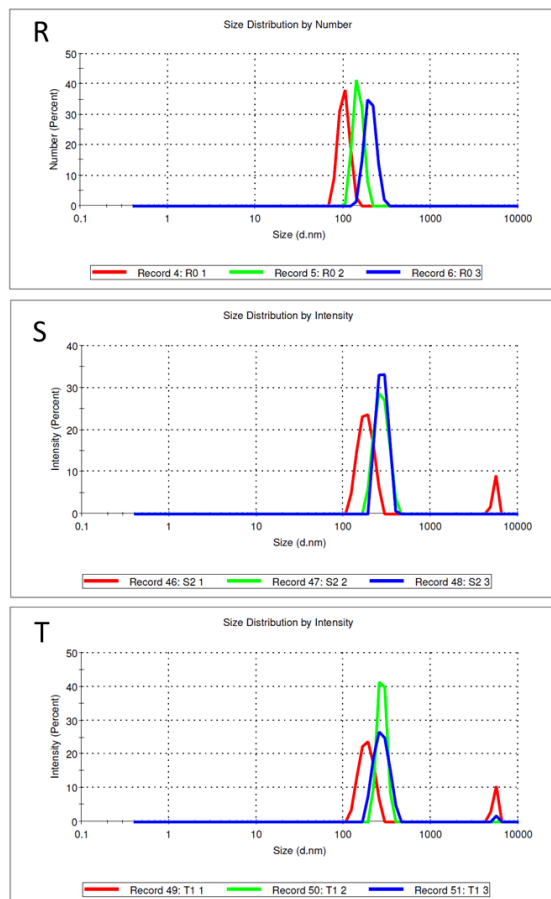


Figure 6 Size distribution of silica nanoparticles by density

3.3. Evaluation of Wettability Properties of Silica/Silane Structures

The contact angle results presented in Figure 7 provide insights into the wettability of the samples. When analyzing the capillary rise method, it's important to consider factors such as particle size, shape, and distribution, as they can influence the wettability of the powder. Previous studies have shown that larger particles tend to have lower contact angles, particularly for liquids with more polar components like water. For instance, Neirinck et. al. [19] investigated the wetting behavior of iron silicide (FeSi) spherical particles and magnetite (Fe₃O₄) irregular particles in different particle size ranges up to

100 μm . They observed a stronger decrease in contact angle with particle size for the spherical particles compared to the irregular particles. The smoother spherical shape contributed to improved wetting behavior, particularly for larger particles.

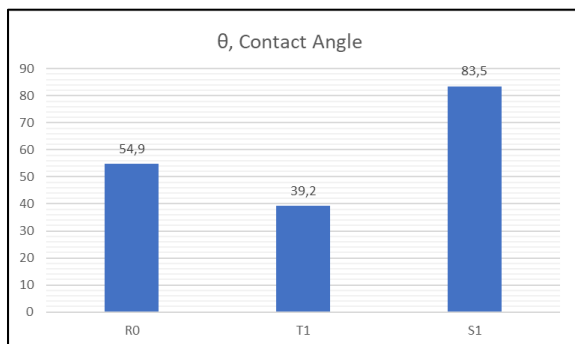


Figure 7 Effect of Silane A-174 on the wettability properties of silica samples

In the context of silica characterization studies, Sample T demonstrated the most favorable results. However, the wettability of silica powders produced by the sol-gel method was found to be very low. Figure 8 illustrates the relationship between contact angle and silica surface area. Generally, as the surface area increases, the contact angle also increases, indicating reduced silaneability properties of silica. This trend is consistent with previous studies in the literature, which have reported a decrease in particle size as surface area increases. Sample T, with its irregular structure, exhibited a lower contact angle compared to samples with a spherical particle structure and higher surface area values. This observation aligns with the Cassie-Baxter equation, which considers heterogeneous wetting and suggests that liquid traps air in surface voids. In this scenario, the contact area between the liquid and solid is minimized, while the area between the liquid and air is maximized. Spherical particles tend to have larger voids compared to irregular particles, allowing for more air to be trapped between the liquid surface and powder surfaces. As a result, the contact angle increases. Higher contact angles indicate lower wettability properties of the powder. Therefore, Sample T demonstrated

higher wettability properties compared to the other samples.

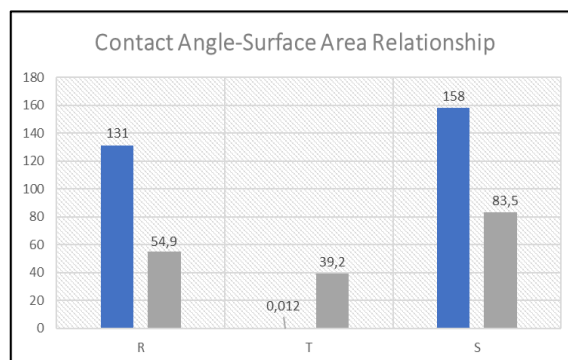


Figure 8 Relationship between contact angle and surface area

3.4. Mechanical Properties of Silica and Silica-Silane Systems Used in Dental Composites

Dental composites cured using blue light are commonly utilized for the restoration of anterior and posterior teeth due to their favorable mechanical properties, clinical performance, and machinability. The addition of a high proportion (>60%) of supporting phase to the composite is done to enhance its performance, where one of the benefits is minimizing polymerization shrinkage by increasing the polymer conversion rate [19].

Polymerization shrinkage and fracture of composite restorations are major factors contributing to clinical failures. Restorative dental composites experience compressive and bending forces, making the evaluation of flexural and compressive strength crucial in determining their mechanical properties. Compressive strength reflects the forces encountered during chewing, while bending strength characterizes the fracture behavior of dental composites, especially in class restorations that are exposed to high forces. Dental composites with high compressive and bending strength not only protect the material against breakage but also safeguard the tooth structure. Although the ISO 4049 Dentistry Polymer-based restorative materials standard does not specify a definite limit for compressive strength, the bending strength is required to be greater than 80 MPa. The

similarity of the mechanical properties of the composite to those of natural teeth is essential in assessing the quality of the composite material.

In the current study, the supporting phase ratios and codes of the produced composites are presented in Table 1. The x-axis represents the type of supporting phase, while the y-axis indicates the percentage of filler. In Table 5, the "*" symbol denotes underloading, and the "***" symbol denotes overloading. The "-" symbol indicates that the sample did not come out of the bending mold and remained in a fragile structure. Based on the codes in Table 1 and the mechanical properties in Table 5, the following composites were deemed liquid due to insufficient loading ratio: C1, C4, C7, C10, C13, and C16. Due to the low light transmittance of C11, C14, and C17 composites, the polymerization process could not be fully realized. Consequently, these composites are not suitable for use as restorative materials due to their poor mechanical properties, and the flexural strength value could not be measured.

Table 5 Mechanical properties of dental composites containing different silica supporting phase and ratio (*: Underloading ratio, **: Overloading ratio, -: samples that do not come out of the bending mold)

	R	R/SA	R/SN	T	T/SA	T/SN	S
σ_e	65	70	*	*	*	*	67
	70	85	98,7	110,2	-	-	**
	75	**	117	125	**	**	**
σ_b	65	*	*	*	*	*	188
	70	288,5	317,2	308,7	-	-	**
	75	**	315,8	352,5	**	**	**

Considering the XRD results of the supporting phase systems produced using the titration method, it is evident that the silica exhibits a crystalline structure. Crystalline structures have tighter grain arrangements, resulting in weaker light transmittance. On the other hand, amorphous structures (non-crystalline) have higher light transmission as they possess interbond spaces. Considering these results, T, T/SA, and T/SN composites

were not utilized as supporting phases in subsequent studies. The S sample had a particle size distribution of 0.1-1 μm . It was observed that the S sample did not possess sufficient bending strength when compared to other supporting phase systems. C3 composite experienced difficulties in gaining consistency and remained in a powder form due to the 75% loading of the supporting phase. In contrast, C9 composite materials exhibited higher mechanical properties compared to other composites.

The composition of the supporting phase, particle geometry and size, as well as their distribution in the composite, significantly affect the physical and mechanical properties of the composite. The higher mechanical properties of the C9 composite in our study can be attributed to the increased content of the supporting phase, which helps minimize polymerization shrinkage and shrinkage stress by reducing the volume of the organic matrix. The interface connection between the matrix phase and the inorganic supporting phases is a crucial element in dental composite fillings. The quality of interfacial bonding directly impacts the mechanical properties of the composite. Poor mechanical adhesion and susceptibility to fracture can occur when there are defects at the interface. To address this issue, the use of silane-based binders is necessary to enhance the interfacial bonding, reduce aggregation of the inorganic supporting phases, and increase the charge of the supporting phase [20].

Examining Table 5, it can be observed that the use of silanated silica significantly improved the mechanical properties. The silanization process was conducted under two different environmental conditions. Silanation in a nitrogen atmosphere, which deprived the environment of oxygen, led to stronger bonding between the -OH groups on the silica surface and the silane agent. This improved interfacial connection resulted in higher mechanical properties exhibited by the C8-C9 composites.

3. CONCLUSION

In this study, we conducted a comprehensive investigation on the impact of different production techniques (Rotary Evaporator, Sol-Gel, and Titration) on the morphology, silanation efficiency, and physical and structural properties of silica nanoparticles. Additionally, we examined the effect of these nanoparticles produced by different methods on the mechanical properties of dental composites. We found that handling smaller particle-sized grains in the Rotary Evaporator technique led to higher loading of silica in dental composites and improved their mechanical properties.

On the other hand, nano silica produced by the sol-gel method exhibited a hydrophobic structure, eliminating the need for silanation. However, this method had the lowest production efficiency, which limited its practical use. The titration method, primarily used for silica sand purification, provided a more economical product with high silane wettability. However, the downside of this method was its long production process, which impacted its applicability compared to the Rotary Evaporator method. Furthermore, the crystal structure and low light transmittance of silica nanoparticles produced by the Titration method hindered the polymerization process and resulted in poor mechanical properties of the composite. Consequently, these composites were not suitable for use as restorative materials, and their flexural strength value could not be measured.

The silanation ability of silica nanoparticles was assessed through contact angle measurements, revealing that nanoparticles obtained by the Titration method exhibited the lowest contact angle. The irregular particle structure contributed to filling the gaps between grains, thereby increasing the silanation properties of the silica nanoparticles.

Considering all the results, it was concluded that nano silica produced using the Rotary Evaporator method was the most suitable for use in dental composites.

Acknowledgments

This study was supported within the scope of TÜBİTAK TEYDEB University-Industry Cooperation project number 5190009 and Yıldız Technical University Scientific Research Project Coordinator's project numbered FYL-2019-3598.

Funding

The authors have not received any financial support for the research, authorship or publication of this study.

Authors' Contribution

The authors contributed equally to the study.

The Declaration of Conflict of Interest/ Common Interest

No conflict of interest or common interest has been declared by the authors.

The Declaration of Ethics Committee Approval

This study does not require ethics committee permission or any special permission.

The Declaration of Research and Publication Ethics

The authors of the paper declare that they comply with the scientific, ethical and quotation rules of SAUJS in all processes of the paper and that they do not make any falsification on the data collected. In addition, they declare that Sakarya University Journal of Science and its editorial board have no responsibility for any ethical violations that may be encountered, and that this study has not been evaluated in any academic publication environment other than Sakarya University Journal of Science.

REFERENCES

- [1] R. K. Ravi, R. K. Alla, M. Shammas, A. Devarhubli, "Dental Composites-A

- Versatile Restorative Material: An Overview.," *Indian Journal of Dental Sciences*, vol. 5, no. 5, 2013.
- [2] M. Sozzi, C. Fornaini, G. Lagori, E. Merigo, A. Cucinotta, P. Vescovi, S. Selleri, "Dental composite polymerization: a three different sources comparison," in *Lasers in Dentistry XXI*, SPIE, 2015, pp. 25–29.
- [3] A. Patodiya, M. N. Hegde, "Dental composites: past, present and future," *National Journal of Community Medicine*, vol. 3, no. 04, pp. 754–756, 2012.
- [4] M. M. Karabela, I. D. Sideridou, "Synthesis and study of properties of dental resin composites with different nanosilica particles size," *Dental materials*, vol. 27, no. 8, pp. 825–835, 2011.
- [5] V. L. Snoeyink, W. J. WEBER JR, "Surface functional groups on carbon and silica," in *Progress in Surface and Membrane Science*, vol. 5, Elsevier, 1972, pp. 63–119.
- [6] J. Jiang, J. Cao, W. Wang, J. Xue, "How silanization influences aggregation and moisture sorption behaviours of silanized silica: analysis of porosity and multilayer moisture adsorption," *Royal Society Open Science*, vol. 5, no. 6, p. 180206, 2018.
- [7] J. P. Matinlinna, C. Y. K. Lung, J. K. H. Tsoi, "Silane adhesion mechanism in dental applications and surface treatments: A review," *Dental materials*, vol. 34, no. 1, pp. 13–28, 2018.
- [8] P. Jiangkongkho, M. Arksornnukit, H. Takahashi, "The synthesis, modification, and application of nanosilica in polymethyl methacrylate denture base," *Dental Materials Journal*, vol. 37, no. 4, pp. 582–591, 2018.
- [9] A. Aydınoglu, A. B. H. Yoruç, "Effects of silane-modified fillers on properties of dental composite resin," *Materials Science and Engineering: C*, vol. 79, pp. 382–389, 2017.
- [10] I. A. Rahman, V. Padavettan, "Synthesis of silica nanoparticles by sol-gel: size-dependent properties, surface modification, and applications in silica-polymer nanocomposites—a review," *Journal of Nanomaterials*, vol. 2012, p. 8, 2012.
- [11] I. A. Rahman, P. Vejayakumaran, C. S. Sipaut, J. Ismail, C. K. Chee, "Effect of the drying techniques on the morphology of silica nanoparticles synthesized via sol-gel process," *Ceramics International*, vol. 34, no. 8, pp. 2059–2066, 2008.
- [12] D.-L. Yang, Q. Sun, H. Niu, R.-L. Wang, D. Wang, J.-X. Wang, "The properties of dental resin composites reinforced with silica colloidal nanoparticle clusters: Effects of heat treatment and filler composition," *Composites Part B: Engineering*, vol. 186, p. 107791, 2020.
- [13] B. Öztürk, M. Yavuz, A. Aydınoglu, O. Güven, A. B. Y. Hazar, "Effect of different drying techniques on silaning efficiency," *Ceramics International*, 2021.
- [14] A. Siebold, A. Walliser, M. Nardin, M. Oppliger, J. Schultz, "Capillary rise for thermodynamic characterization of solid particle surface," *Journal of Colloid and Interface Science*, vol. 186, no. 1, pp. 60–70, 1997.
- [15] M. O. Kangal, G. Bulut, O. Guven, "Physicochemical characterization of

- natural wollastonite and calcite,” *Minerals*, vol. 10, no. 3, p. 228, 2020.
- [16] I. M. Joni, L. Nulhakim, M. Vanitha, C. Panatarani, “Characteristics of crystalline silica (SiO_2) particles prepared by simple solution method using sodium silicate (Na_2SiO_3) precursor,” in *Journal of Physics: Conference Series*, IOP Publishing, 2018, p. 012006.
- [17] Y. Wang, Q. Zhao, N. Han, L. Bai, J. Li, J. Liu, E. Che, L. Hu, Q. Zhang, T. Jiang, S. Wang “Mesoporous silica nanoparticles in drug delivery and biomedical applications,” *Nanomedicine*, vol. 11, no. 2, pp. 313–327, 2015.
- [18] R. A. Bakar, R. Yahya, S. N. Gan, “Production of high purity amorphous silica from rice husk,” *Procedia Chemistry*, vol. 19, pp. 189–195, 2016.
- [19] B. Neirinck, J. Van Deursen, O. Van der Biest, J. Vleugels, “Wettability assessment of submicrometer alumina powder using a modified washburn method,” *Journal of the American Ceramic Society*, vol. 93, no. 9, pp. 2515–2518, 2010.
- [20] H. A. Rodríguez, W. M. Kriven, H. Casanova, “Development of mechanical properties in dental resin composite: Effect of filler size and filler aggregation state,” *Materials Science and Engineering: C*, vol. 101, pp. 274–282, 2019.